

University of Pardubice  
Faculty of Chemical Technology  
Institute of Chemistry and Technology  
of Macromolecular Materials

**PREPARATION OF MONODISPERSE POLYMER  
MICROSPHERES WITH SURFACE REDUCING  
NONSPECIFIC PROTEIN ADSORPTION**

*Annotation of Ph.D. Thesis*

*Author: Jana Koubková*

*Supervisor: Daniel Horák, Ph.D.*

## ABSTRACT

With the aim to develop micrometer-sized monodisperse polymer particles with surface minimizing nonspecific protein adsorption, polyzwitterion-modified microspheres were prepared. Simultaneously, effect of the surface modification on structure and properties of the microspheres was investigated. Starting poly(glycidyl methacrylate) particles, size of which was controlled in range 0.5-5.5  $\mu\text{m}$ , were prepared by the dispersion polymerization. During the synthesis, influence of many reaction parameters, e.g., polarity of the reaction mixture, type of the co-solvent, molecular weight and concentration of the stabilizer, concentration of the monomer and the initiator and reaction temperature, on the particle morphology, size and size distribution was determined. First, the polymer microspheres were functionalized with chain transfer agent in order to perform surface-initiated polymerization of the zwitterion. The chain transfer agent was attached via three different ways and the optimal approach was found. Moreover, the amount of immobilized chain transfer agent relative to reactive groups and properties of the activated particles were optimized. Subsequently, effect of the solvent on the amount of grafted zwitterionic polymer was confirmed. Up to 20 wt.% of zwitterionic polymer was attached to the particle surface. Polyzwitterion-modified microspheres were characterized by commonly available physico-chemical methods and the resistance to nonspecific protein adsorption was verified using bovine serum albumin as a model protein.

**Key words:** poly(glycidyl methacrylate), dispersion polymerization, zwitterion, RAFT polymerization, nonspecific protein adsorption

# CONTENT

<b>1. Introduction</b> .....	3
<b>2. Theoretical part</b> .....	3
2.1 Preparation of polymer microspheres .....	3
2.1.1 Suspension polymerization .....	3
2.1.2 Emulsion polymerization .....	4
2.1.3 Dispersion polymerization .....	5
2.1.4 Precipitation polymerization.....	6
2.1.5 Multistep swelling polymerization .....	6
2.2 Surface modification of polymer microspheres .....	6
2.2.1 Nitroxide mediated polymerization .....	7
2.2.2 Atom transfer radical polymerization .....	7
2.2.3 Reversible addition-fragmentation chain transfer polymerization .....	7
2.3 Materials reducing nonspecific protein adsorption.....	9
2.3.1 Polymer brushes based on neutral polymers.....	9
2.3.2 Polymer brushes based on ionic polymers .....	9
2.4 Characterization of polymer microspheres .....	10
2.4.1 Morphology, size and size distribution.....	10
2.4.2 ATR FTIR spectroscopy .....	10
2.4.3 Surface charge.....	10
<b>3. Aim of the study</b> .....	11
<b>4. Experimental part</b> .....	11
4.1 Dispersion polymerization.....	11
4.2 Surface-initiated RAFT polymerization .....	11
4.3 Nonspecific protein adsorption .....	12
<b>5. Results and discussion</b> .....	12
5.1 Preparation of polymer microspheres .....	12
5.2 Attachment of dithiobenzoic acid to the particle surface .....	16
5.3 Surface-initiated RAFT polymerization .....	19
5.4 Characterization of RAFT polymerization of MPDSAHA.....	22
5.5 Characterization of surface-modified PDHPMA microspheres.....	23
5.6 Nonspecific protein adsorption on microspheres .....	25
<b>6. Conclusions</b> .....	26
<b>7. List of abbreviations</b> .....	27
<b>8. References</b> .....	29
<b>9. List of author publications</b> .....	32

# 1. INTRODUCTION

Polymer microspheres are widely used in many industrial applications for long periods of time. Their first applications included ion exchangers and separations of heavy metals from waste water [1]. With the development of new polymerization methods, synthesis of the polymer microspheres was gradually improved and uniform microspheres of well-defined size and size distribution were obtained. Nowadays, such particles are used as stationary phases in chromatographic columns, in electrophoretic techniques and increasingly also in biological and biomedical applications [2,3].

During separations of biomolecules from the real samples, affinity of the separated compound to surface of the polymer microspheres has to be ensured and simultaneously, the polymer microspheres must resist nonspecific adsorption of other undesirable substances. Thus, surface of the polymer particles has to be modified with proper compounds including macromolecules. Electroneutral hydrophilic polymers belong among the commonly used substances, however, promising results have been achieved also with the surfaces modified by polymers possessing both positive and negative charges [4]. Pseudo-living radical polymerizations are very often used for anchoring the polymer chains on the modified surface [5,6].

Polymer microspheres must be chemically stable, contain reactive functional groups, exhibit minimal nonspecific protein adsorption and must not aggregate. Regular spherical shape, narrow particle size distribution and size of the polymer microspheres play also a key role. The size between 2 and 10  $\mu\text{m}$  is suitable for many biological applications since such microspheres provide sufficiently large surface area for interactions with separated compounds and enhance the separation efficiency. The narrow particle size distribution then ensures uniform physical, chemical and biological properties.

## 2. THEORETICAL PART

### 2.1 Preparation of polymer particles

Polymer particles are predominantly produced by heterogeneous polymerizations consisting of two separated phases. The two-phase system can be formed either at the beginning of the polymerization, when monomer is insoluble in the reaction medium under formation of separated liquid phase, or during the polymerization, when the growing polymer chains become insoluble and precipitate from the reaction mixture. Most of the heterogeneous polymerization systems are initiated by thermal decomposition of initiators at high temperature. Typical initiators are peroxidic compounds or azo-compounds including 2,2'-azobis(2-methyl-propionitril) (AIBN) or 4,4'-azobis(4-cyano-pentanoic acid) (ACVA).

#### 2.1.1 Suspension polymerization

Suspension polymerization is the oldest technique used for preparation of the polymer microspheres, size of which ranges from tens of micrometers up to 1–2 mm [7]. In the suspension polymerization, the monomer phase with dissolved initiator is suspended in an

immiscible polymerization medium (usually water) in the form of microdroplets. Individual monomer droplets represent tiny reactors, in which the polymerization proceeds, and the suspension medium acts as an efficient heat transfer agent [7]. On the basis of these minireactors, the polymerization kinetic is similar to that of the bulk polymerization [7]. Suspension polymerization requires addition of small amounts of a stabilizer to hinder droplet coalescence and droplet break-up during the polymerization. Typical droplet stabilizers include polymers, such as poly(*N*-vinyl-pyrrolidone) (PVP), polyvinylalcohol, poly(acrylic acid) (PAA) and cellulose derivatives, or colloid inorganic solutions [8]. The stabilizer is adsorbed on the droplet surface, decreases the interfacial tension, which contributes to formation of small droplets and prevents their breaking-up. When the balance between the droplet break-up and their repeated coalescence is achieved, microspheres with a narrow size distribution are produced. The main disadvantage of microspheres prepared by the suspension polymerization is their relatively broad particle size distribution.

### **2.1.2 Emulsion polymerization**

Emulsion polymerization has been known since the 1930s, however, only in the late 1940s the theoretical basis was established [9]. Emulsion polymerization is convenient method for preparation of monodisperse submicrometer particles [7]. Usually, the monomer, which is sparingly soluble in water, is emulsified in a continuous aqueous phase with the aid of an emulsifier (surfactant). The emulsifier contains hydrophilic and hydrophobic part. While the hydrophobic part adsorbs on the surface of monomer droplets, the hydrophilic part is oriented into the aqueous phase. Size of the monomer droplets (*ca.* 1–10  $\mu\text{m}$ ) is significantly larger than size of the final polymer particles. Emulsion polymerization process can be classified into three stages. At the beginning of the polymerization, initiation in the aqueous phase and nucleation of the polymer particles take place. The second stage is characterized by the constant monomer concentration and by the particle growth. In the third stage, the monomer droplets disappear, concentration of the monomer in the polymer particles decreases and the polymerization slows down.

The nucleation process depends on the monomer being polymerized and on the emulsifier concentration. If the concentration exceeds a certain limit, so called critical micellar concentration (CMC), first micelles appear [10]. When a water-insoluble monomer is used and the emulsifier concentration is  $>$  CMC, the polymerization is initiated in the monomer-swollen micelles by capture of a free radical. During the polymerization, the monomer in the micelles is being consumed and refilled from the monomer droplets in which the polymerization has not started yet [11,12]. According to the theory of homogeneous nucleation (applicable for monomers partly soluble in water or for emulsifier concentrations  $<$  CMC), the polymerization begins in the aqueous phase [12,13]. The oligomer radicals grow until they reach a critical chain length, when they become insoluble and precipitate into polymer particles. This mechanism is discussed in chapter 2.1.3.

### 2.1.3 Dispersion polymerization

Dispersion polymerization was discovered at the beginning of the 1970s [14]. Firstly, it was carried out in nonpolar, later in polar solvents including alcohols, mixtures of alcohols and mixtures of alcohols with ethers [14]. At the beginning, the polymerization mixture forms homogenous solution containing dissolved initiator, monomer and polymer stabilizer. The primary particles in the dispersion polymerization are formed via homogeneous nucleation (Figure 1). Free radicals generated in continuous phase react with the monomer units and form growing oligomer chains. Upon reaching a critical chain length, the oligomer radicals become insoluble and precipitate under the formation of small unstable nuclei. Two different models of the particle nucleation have been proposed [14]:

- *self-nucleation* – the oligomer chains grow in the solution until they reach a critical chain length and collapse into a condensed state ( $\sim$  particle nuclei);
- *aggregative nucleation* – growing oligomer chains associate with each other as their molecular weight and concentration rise. Aggregates below a certain size are unstable, but above this size they become stable and continue in growth.

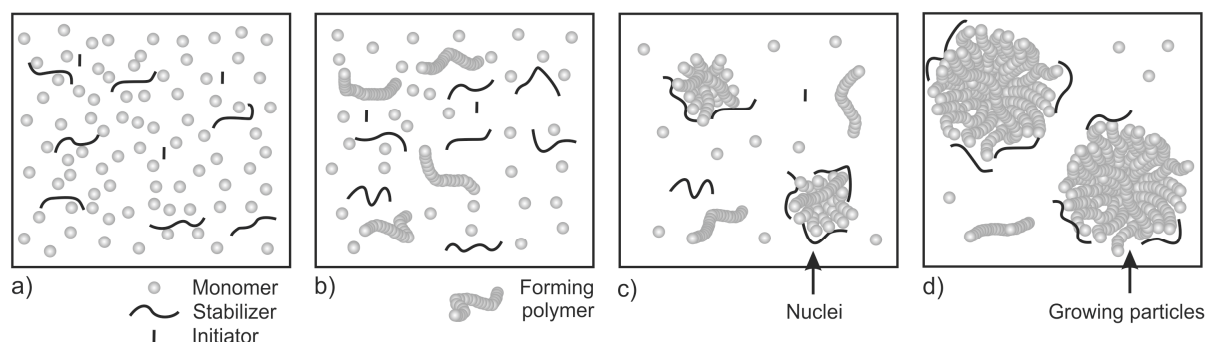


**Figure 1.** Mechanism of dispersion polymerization. Monomer, initiator and stabilizer are dissolved in the polymerization medium (a), oligomers soluble in the polymerization medium are formed (b), nucleation occurs (c) and the particles grow by capturing of monomer and oligomers from the continuous phase (d) [15].

The nuclei, typically 15–20 nm in size [16], are unstable until enough of the polymer stabilizer is adsorbed on their surface. Once a sufficient amount of stable primary particles is formed, nucleation process is completed. The polymer particles capture monomer and most of the oligomer from the continuous phase before the oligomer chains will reach the critical length. The main locus of the polymerization is transferred to the polymer particles which continue to grow [14,16]. Due to the continuing polymerization, viscosity in the polymer microspheres increases, which hinders motion of the polymer radicals, however, diffusion of the monomer is preserved. Therefore, the propagation continues with the unchanged rate unlike the termination, rate of which is decreased due to the limited motion of polymer radicals. As a consequence, the propagation rate and the molecular weight of the polymer chains increase. This phenomenon is known as gel effect and is typical for polymerizations of nonpolar monomers in polar solvents [14].

The critical chain length is determined by the medium polarity and thus by the solubility of the polymer in the continuous phase [17]. Besides, the polymer solubility is influenced by the monomer concentration. As most of the polymers are well-soluble in their own mono-

mers, with its growing concentration in the mixture the polymer solubility, and as a consequence, the critical chain length and particle size increases [18]. However, the dispersion polymerization and size of the final polymer particles are influenced by other reaction parameters including the type and concentration of the initiator, reaction temperature, etc. [16,17].

#### **2.1.4 Precipitation polymerization**

Mechanism of the precipitation polymerization is an analogy of that of the dispersion polymerization. Monomer and initiator are in the form of a homogeneous solution in an appropriate solvent. However, the polymerization is carried out in the absence of any stabilizer. After precipitation of the oligomer chains, the particle nuclei are stabilized by a layer of oligomers swollen with the polymerization medium. The polymerization takes place at the particle-solvent interface [15].

#### **2.1.5 Multistep swelling polymerization**

Multistep swelling polymerization provides monodisperse polymer microspheres in the size range 1–20  $\mu\text{m}$  [15]. The method consists in swelling of preformed, monodisperse polymer seeds, which are firstly activated (pre-swollen) with a water-insoluble liquid. Subsequently, the activated seeds are swollen with a monomer, mixture of monomers or mixture of monomers and a porogen [19]. During the swelling process, each polymer seed is equally swollen, which ensures production of highly monodisperse polymer microspheres [19].

### **2.2 Surface modification of polymer microspheres**

In general, polymer materials are modified to improve their surface properties, such as wettability, adhesion, biocompatibility, controlled cell and protein adsorption, reduced nonspecific protein adsorption, etc. Modification with the macromolecular compounds uses structure of polymer brushes, which are assemblies of the polymer chains attached by one end to the modified surface and stretched to the medium [6,20]. Polymer brushes can be anchored either reversibly via physisorption, or irreversibly via chemical bonding. Physisorption of surface-active polymer chains from thermodynamically poor solvents presents easy approach of chain binding. However, the polymer brushes exhibit thermal and solvolytic instability and desorption can occur upon exposure to good solvents, or the adsorbed polymers can be displaced by low-molecular compounds, or other polymers [20]. Some of these drawbacks can be overcome by covalent attachment of the polymer chains, which can be done by two main approaches:

- *grafting to* – preformed, end-functionalized polymers react with suitable groups on the substrate surface and form a polymer brush. However, due to the steric barrier caused by previously grafted chains, the grafting density and film thickness is restricted;

- *grafting from* – the initiator is immobilized onto the surface followed by surface-initiated polymerization to generate tethered polymers. This method allows preparation of relatively dense polymer brushes, however, multistep synthesis is necessary [6,20].

Both approaches can be accomplished via ionic, conventional radical or so-called pseudo-living radical polymerization mechanism. In order to achieve a better control of molecular weight and its distribution, pseudo-living techniques attract more attention. The techniques described below belong among the most important controlled polymerization methods [5].

### 2.2.1 Nitroxide mediated polymerization

Mechanism of nitroxide mediated polymerization (NMP) is based on a reversible termination of the growing polymer chains by nitroxide [21,22]. The thermal decomposition of C–O bond in alkoxyamine initiator produces two radical centers: initiating transient and persistent nitroxide radical. The transient radical reacts with monomer units until it is deactivated with nitroxide radical. At the beginning of the reaction, the transient radicals react with each other leading to their irreversible termination and an increased concentration of persistent nitroxide radicals that cannot undergo irreversible termination. The small excess of persistent radicals ensures an effective deactivation of growing polymer chains and thus a controlled growth of molecular weight [21,22].

### 2.2.2 Atom transfer radical polymerization

The key reaction in atom transfer radical polymerization (ATRP) is the reversible transfer of a halogen atom between an initiator (typically alkyl halides RX) and a transition metal complex  $M^nX_nL_m$  as a catalyst, where M is the transition metal, X halogen and L ligand [23]. After homolytic cleavage of R–X bond in the alkyl halide, a free carbon-centered radical and the halogen atom are generated. The halogen atom transfers to the metal complex and oxidizes it to higher oxidative state  $M^{n+1}X_{n+1}L_m$ . Free radicals propagate with monomer in the solution until after addition of several monomer units are deactivated with transient metal complex in the oxidative state  $M^{n+1}X_{n+1}L_m$ . The bond R–X is recovered and polymer chains are transferred into a dormant state. Fast activation and deactivation of growing polymer radicals ensures the uniform growth of chains and their narrow molecular weight distribution [23,24]. The main drawback of ATRP polymerization is the residual traces of transient metal complexes in final products, which may limit their application in biomedical or electronic industry.

### 2.2.3 Reversible addition-fragmentation chain transfer polymerization

Reversible addition-fragmentation chain transfer polymerization (RAFT) consists in an introduction of a small amount of chain transfer agent (CTA) in a conventional free-radical system [25,26]. The transfer of CTA between growing radicals and dormant polymer chains regulates the growth of molecular weight [25,26]. The mechanism of RAFT polymerization is shown in Figure 2. The free radicals generated by the initiator decomposition react with the monomer (Figure 2; I). These growing radical chains rapidly add to the reactive C=S bond of

the CTA to form a radical intermediate. The reversible fragmentation of radical intermediate occurs either toward the initial growing chain or to provide the reinitiating R group and a polymer CTA, so called macro-CTA (Figure 2, II). The R group can reinitiate polymerization by reacting with the monomer and form a new polymer chain (Figure 2, III), which continues in growth or reacts back on the macro-CTA. Once the initial CTA is consumed, the macro-CTA is mainly present in the polymerization medium and an equilibrium in rapid exchange between active and dormant chains is achieved (Figure 2; IV). This equilibrium is considered as the main equilibrium ensuring equal probability for all chains to grow and thus leading to polymers with narrow molecular weight distribution. The irreversible radical termination is not avoided (Figure 2, V), however, these reaction are kept to a minimum. The final product contains a majority of polymer chains having the reinitiating R group at one end and thiocarbonyl-thio group at the other [25,26].

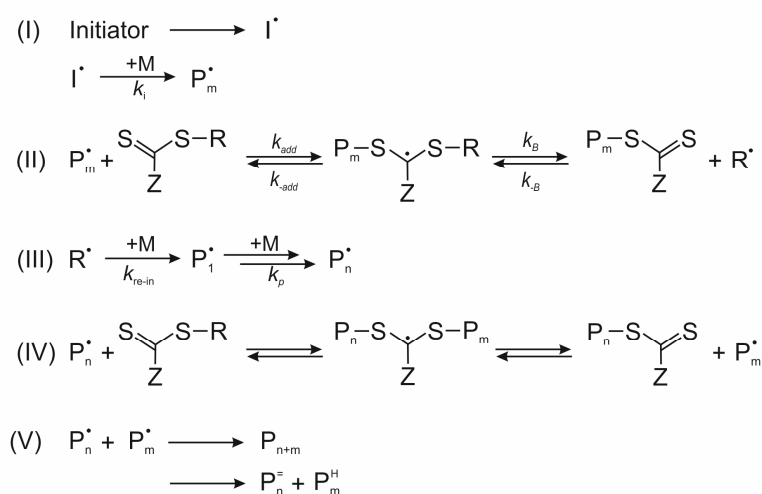


**Figure 2.** Proposed mechanism of RAFT polymerization [26]

The reactivity of CTA is determined by the character of R and Z groups. The Z group influences stability of the radical intermediate, and thus, determines the reactivity of C=S bond toward radical addition. However, the radical intermediate cannot be too stable to allow fragmentation and cleavage of reinitiating R group. Benzyl and phenyl groups were found as the suitable Z groups for most monomers [25,26]. On the other hand, R group must be a good leaving group in comparison with the growing polymer chain and good reinitiating group toward the monomer [26]. Commonly CTAs used in RAFT polymerization include dithioesters (mainly dithiobenzoates with Z = phenyl), xanthates, trithiocarbonates, etc. [25,26]. The choice of CTA depends on the monomer being polymerized.

Surface-initiated RAFT polymerization can be performed using two different approaches [6,25]:

- *surface-anchored initiator* – these reactions include mostly conventional free azo-initiators;
- *surface-anchored chain transfer agent* – the CTA can be attached either via its leaving R or stabilizing Z group.

The R-group approach resembles the “grafting from” process. The solid surface acts as a part of the R groups, the propagating radicals are located on the terminal end of the surface-

grafted polymer [6,25]. In Z-group approach, the CTA is permanently attached to the surfaces, polymer radicals propagate in solution before they attach to the surface. However, due to the steric barrier of the neighboring attached chains, the grafting density can be restricted [6,25]. Both approaches have been used for modification of numerous surfaces including, e.g., of poly(divinylbenzene) microspheres with styrene using 1-phenylethyl dithiobenzoate [27].

## 2.3 Materials reducing nonspecific protein adsorption

Surfaces resistant to nonspecific interactions are required in many biotechnological applications. Protein fouling can impair functions of various biotechnological and biomedical devices by stopping flow through porous membranes, false response of a biosensor, etc. [28]. The requirements laid on antifouling surfaces include mainly wettability, hydrophilicity and neutral charge [28].

### 2.3.1 Polymer brushes based on neutral polymers

Poly(ethylene glycol) (PEG) is a hydrophilic polymer frequently used in prevention of protein adsorption and cell adhesion. The resistance is ensured by PEG conformational flexibility, steric repulsion and formation of hydration water layer that hinders penetration of proteins to the surface [29]. The weak point of PEG is its low thermal stability at temperatures  $> 36\text{ }^{\circ}\text{C}$ , when it loses its ability to resist nonspecific protein adsorption [30].

### 2.3.2 Polymer brushes based on ionic polymers

Polymer brushes containing charged groups can be prepared either by copolymerization of monomers possessing anionic and cationic groups on separated units, or by polymerization of zwitterions containing both negatively and positively charged groups within the same monomer unit [31]. According to the anionic moiety, the zwitterions can be classified into three main categories: carboxy- (possessing carboxylate group), phospho- (mostly with phosphate group) and sulfobetaines having sulfonate as the negatively charged group (Figure 3); the cationic moiety is mostly quaternary ammonium group [31].

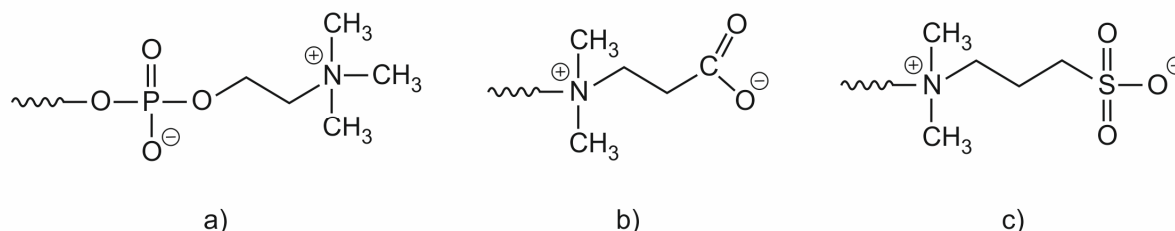


**Figure 3.** General structure of phospho- (a), carboxy- (b) and sulfobetaines (c) [38].

The mechanism of polyelectrolyte resistance differs from that of PEG. While hydroxyl groups of PEG bind the water molecules via the hydrogen bonds and thus form the hydration layer, polyelectrolytes electrostatically interact with water molecules [32]. Ability to

resist the nonspecific protein adsorption is influenced by the character of anionic groups, distance between both charged functionalities and also by the type of polymerizable terminus of the zwitterions [6,33,34].

## 2.4 Characterization of polymer microspheres

### 2.4.1 Morphology, size and size distribution

The microsphere size, shape and size distribution, surface character and aggregation can be observed by scanning electron microscopy (SEM). In this study, SEM micrographs were taken on a JEOL JFM 6400 (Tokio, Japan) and analyzed by software Atlas (Tescan, Brno, Czech Republic). The particle size and distribution was calculated according to the following equations:

$$D_n = \sum D_i / N \quad (1)$$

$$D_w = \sum D_i^4 / \sum D_i^3 \quad (2)$$

$$PDI = D_w / D_n \quad (3),$$

where  $D_i$  is diameter of an individual microsphere,  $N$  is number of the particles (at least 800),  $D_n$  and  $D_w$  are number-average and weight-average diameter and  $PDI$  is polydispersity index characterizing the particle size distribution.

### 2.4.2 ATR FTIR spectroscopy

Thin surface layer can be characterized by Fourier transform infrared spectroscopy performed in an attenuated total reflectance mode (ATR FTIR). The method uses property of total internal reflection at the interface of the sample and the ATR crystal with a high refractive index [35]. The measurement was carried out on a Thermo Nicolet NEXUS 870 FTIR spectrometer (Madison, USA). Spectra of the powdered samples were measured with a Golden Gate™ Heated Diamond ATR Top-Plate (Specac; Orprington, UK). Typical conditions were: 256 sample scans, resolution 4 cm<sup>-1</sup> and wavenumber range 400–4000 cm<sup>-1</sup>.

### 2.4.3 Surface charge

Net charge at the particle surface influences the distribution of ions in the particle surroundings, resulting in an increased concentration of counter ions (of opposite charge to that of the particle) close to the particle surface. Thus, an electrical double layer exists around each particle. The zeta ( $\xi$ ) potential expresses the potential of slipping plane formed between an ionic layer moving with the particle and layer of ions which do not travel with the particle. The  $\xi$  potential was measured on a Zeta-Sizer Nano-ZS model ZEN3600 (Malvern Instruments; Malvern, UK) and calculated by the Malvern software using Henry's equation (4):

$$\xi = (3\eta U_E) / (2\varepsilon f_{(Ka)}) \quad (4),$$

where  $U_E$  is electrophoretic mobility,  $\eta$  is viscosity of the solvent,  $\varepsilon$  its dielectric constant and  $f_{(Ka)}$  is Henry's function that was expressed by Smoluchowski approximation ( $f_{(Ka)} = 1.5$ ). This approximation is valid for large particles with a thin double-layer [36].

### 3. AIM OF THE STUDY

Aim of this thesis is to develop new polymer microspheres with surface preventing nonspecific protein adsorption. Predominantly, the microsphere size and the particle size distribution are strongly influenced by the polymerization conditions. In the first part of the thesis, the aim was to determine effect of some reaction parameters on the dispersion polymerization of glycidyl methacrylate (GMA) and morphology, size and size distribution of the final poly(glycidyl methacrylate)(PGMA) microspheres. The next objective was to activate the microspheres with chain transfer agent (CTA) to enable modification of the particle surface. More specifically, effect of attachment of dithiobenzoic acid (DTBA) as the suitable CTA had to be found and the optimal approach of the attachment had to be determined. Another objective was to develop surface-initiated reversible addition-fragmentation chain transfer (RAFT) polymerization from the PGMA microspheres under different reaction conditions, e.g., solvent system, monomer concentration. Last but not least, the zwitterion-modified PGMA microspheres had to be characterized and their resistance to nonspecific protein adsorption evaluated.

### 4. EXPERIMENTAL PART

#### 4.1 Dispersion polymerization

In a typical experiment, 0.32 g of poly(acrylic acid) (PAA) was dissolved in 50 g of ethanol (EtOH), EtOH/2-ethoxyethanol (EtCel) or EtOH/water mixture and charged into a 70-ml reaction vessel together with a solution of 0.176 g of 2,2'-azobis(2-methylpropionitrile) (AIBN) in 3.82 g of GMA. The reaction mixture was purged with nitrogen and the polymerization was started by heating at 70 °C for 16 h under stirring (400 rpm). Final PGMA microspheres were ten times washed with distilled water.

#### 4.2 Surface-initiated RAFT polymerization

Prior to immobilization of CTA, a part of the PGMA microspheres (1 g) was hydrolyzed in 0.1M H<sub>2</sub>SO<sub>4</sub>, or ammonolyzed in 25% aqueous ammonia solution. An ATRP initiator,  $\alpha$ -bromoisobutyryl bromide (BIBB), was reacted with hydrolyzed or ammonolyzed microspheres at several BIBB/OH or BIBB/NH<sub>2</sub> molar ratios, respectively. Chain transfer agent, dithiobenzoic acid (DTBA), was attached to the BIBB-activated microspheres (DTBA/Br = 1:1 mol/mol), as well as to the initial PGMA microspheres at several DTBA/oxirane molar ratios. Surface-initiated RAFT polymerization of zwitterion [3-(methacryloylamino)propyl]-dimethyl(3-sulfopropyl)ammonium hydroxide (MPDSAHA), typically 0.4 g, was carried out in 4 ml of reaction solvent (water, acetic buffer, methanol (MeOH), EtOH) containing 4,4'-azobis(4-cyanopentanoic acid) (ACVA) as an initiator. The reaction mixture was purged with argon, closed with rubber septum and degassed (vacuum, - 80 °C) and again purged with argon. The polymerization was started by heating at either 60 °C (MeOH) or 70 °C (water, EtOH) for 20 h under stirring (400 rpm). The resulting surface-modified PDHPMA-PMPDSAHA microspheres were repeatedly washed with water and phosphate buffer (PBS).

### 4.3 Nonspecific protein adsorption

To verify antifouling properties of the PDHPMA-PMPDSAHA microspheres, adsorption of proteins was investigated using bovine serum albumin (BSA) as a model. Solution of BSA in PBS (1.8 ml; 2 mg/ml) was added to the PDHPMA-PMPDSAHA microspheres (18 mg) and the mixture incubated for 2 h at 20 °C under stirring (50 rpm). After the incubation, the mixture was centrifuged, supernatant separated and analyzed using a UV/VIS spectrometer Biochrom Libra S22 (Cambridge, UK). Concentration of BSA in the sample was calculated from a calibration curve, compared with the original amount of BSA in the solution and amount of BSA adsorbed on the microspheres was determined.

## 5. RESULTS AND DISCUSSION

### 5.1 Preparation of polymer microspheres

Dispersion polymerization is considered as a convenient method for preparation of the micrometer-sized polymer particles of a narrow size distribution. However, morphology, size and polydispersity of the polymer microspheres are influenced by a number of reaction parameters including polarity of the solvent system, type and concentration of the stabilizer and the initiator, composition of the monomer mixture and the reaction temperature.

#### *Effect of solvent system*

Solvency of the dispersion medium for the polymer is one of the key parameters influencing the particle formation. The solvency of the reaction mixture was estimated by averaging the solubility parameters  $\delta$  of the reaction components according to equation 5:

$$\delta = (\sum(v_i\delta_i^2))^{1/2} \quad (5),$$

where  $v_i$  and  $\delta_i$  represent the volume fraction and solubility parameter of the component  $i$ , respectively. Contribution of the polymer stabilizer, the initiator and the polymer produced was not included.

First, PAA-stabilized dispersion polymerization was carried out in EtOH/EtCel mixture. The PGMA microsphere size slightly increased with decreasing solubility parameter, i.e., with higher EtCel contents (Figure 4 a). Similarly to *N,N*-dimethylformamide (DMF), EtCel is a thermodynamically better solvent for PGMA than EtOH [37]. Therefore, with increasing content of EtCel in the mixture the solubility of the oligomer chains was higher and PGMA nuclei precipitated at a later polymerization stage [37]. The PGMA microspheres were larger, however, their number was reduced than if the precipitation occurred from the neat EtOH.

Exactly the opposite dependence was observed for the polymerization of GMA in EtOH/water mixture. Size of the PGMA microspheres increased significantly with increasing solubility parameter of the reaction mixture (Figure 4 b). Water is thermodynamically poorer solvent for PGMA than neat EtOH. Thus, at higher water contents (i.e., at a higher solubility parameter), the oligomer chains should precipitate upon reaching relatively short critical chain length allowing formation of small particles. However, water is good solvent

for PAA stabilizer and thus hinders PAA adsorption, as well as formation of PAA-*graft*-PGMA copolymers [16]. Besides, majority of the monomer is present inside the growing polymer particles. Due to a higher polymerization rate, the particles will grow into larger size than the same particles prepared only in EtOH [38].

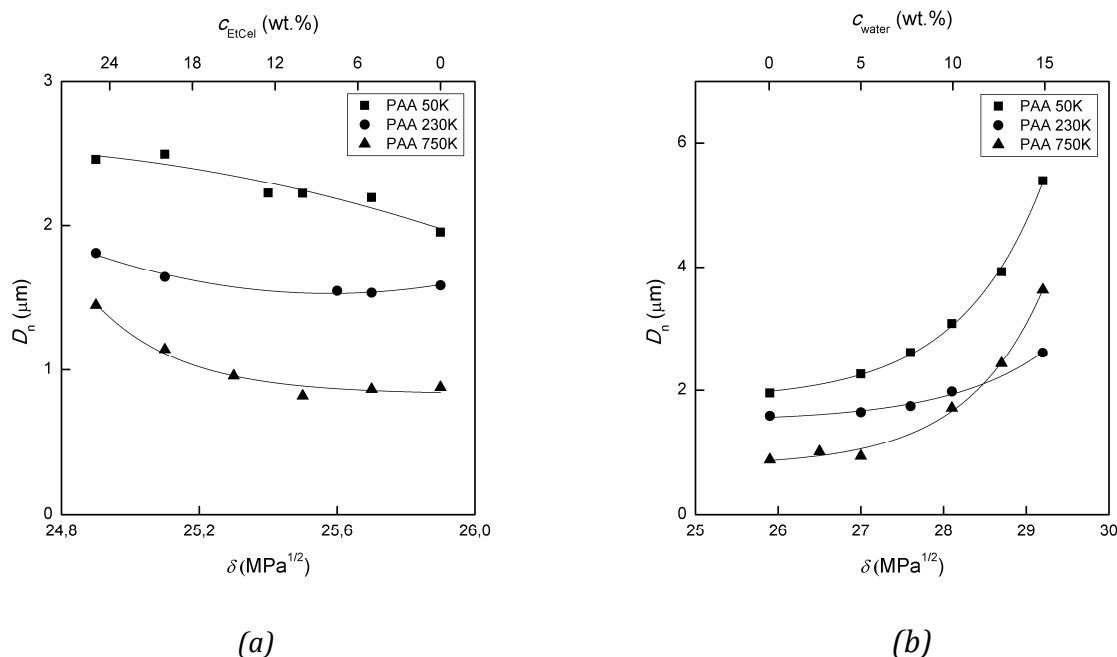


**Figure 4.** Dependence of the PGMA microsphere diameter  $D_n$  on the solubility parameter  $\delta$  of EtOH/EtCel (a) and EtOH/water mixture (b).

### Effect of stabilizer

In the present system, PAA was chosen as a steric stabilizer mainly due to its solubility in alcoholic and water media. Besides, PAA contains  $\alpha$ -hydrogens capable of graft copolymer (PGMA-*graft*-PAA) formation. This *in situ* formed graft copolymer participates together with precursor PAA in the stabilizing process. Properties of the PGMA microspheres are affected not only by chemical structure of the stabilizer, but also by its molecular weight. Thus, PAAs of three molecular weights ( $M_w = 50,000$ ; 230,000 and 750,000) were used in the experiments. With increasing molecular weight of the stabilizer, the particle size decreased (Figure 5). As high-molecular-weight PAA was capable to stabilize larger surface area, size of the final particles was smaller than in the systems containing low-molecular-weight stabilizers [37,39]. Besides, increased viscosity of medium containing high-molecular-weight PAA limited nuclei aggregation and smaller PGMA microspheres were thus formed.

Increase of the PAA concentration in the reaction mixture caused both higher medium viscosity and higher adsorption rate of PAA and PAA-*graft*-PGMA stabilizers [38]. As more stabilizer molecules were adsorbed on the particle surface, the nuclei aggregation was reduced, number of the stable particles enhanced and as a result, small particles were produced [37] (Figure 5). Control of the PAA-stabilized microsphere size was more effective than in case of PVP-stabilized PGMA microspheres (Figure 5).

It is necessary to note that stabilization with both medium-molecular-weight PAAs ( $M_w = 50,000$  and 230,000) led to production of regular and monodisperse PGMA microspheres

(PDI < 1.05) in most cases (Figure 6 a, b). On the contrary, particle size distribution of the PGMA microspheres stabilized with PAA ( $M_w = 750,000$ ) was much broader and monodisperse particles were not obtained in any of the studied systems (Figure 6 c).

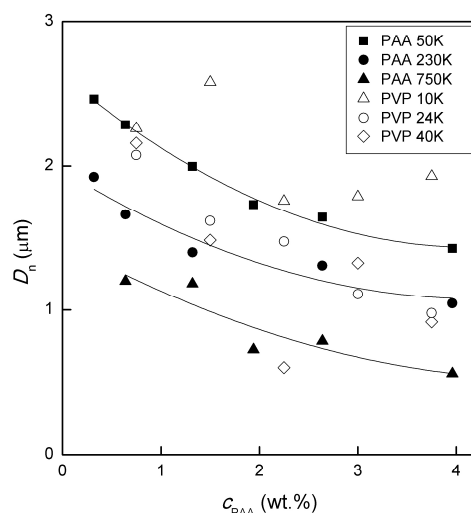


**Figure 5.** Dependence of the PGMA microsphere diameter  $D_n$  on the concentration  $c$  and molecular weight of PAA and PVP used as stabilizer. Data for PVP were taken from [37].

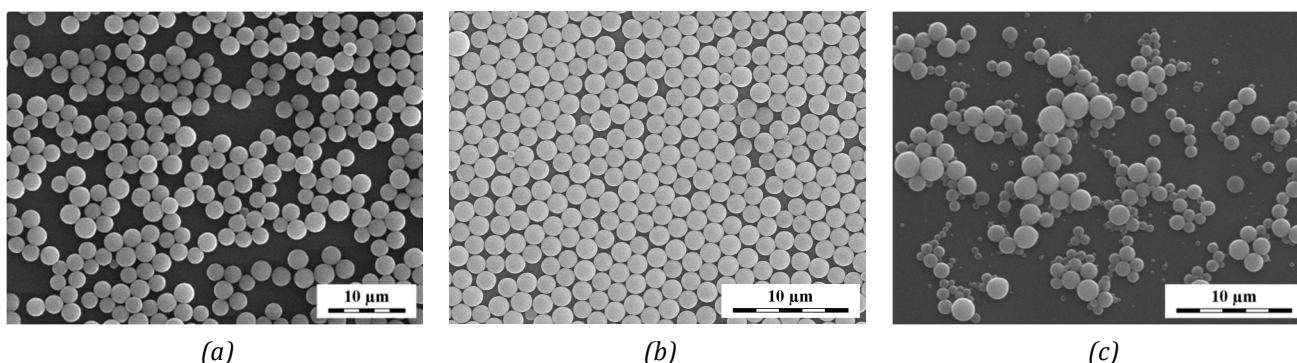


**Figure 6.** SEM micrographs of PGMA microspheres stabilized with PAA of  $M_w = 50,000$  (a),  $230,000$  (b) and  $750,000$  (c).

### Effect of monomer concentration

The monomer concentration can influence the particle size in several ways, often with contrary impacts. In this set of experiments, the dependence of PGMA microsphere size on GMA concentration passed through a minimum ranging from 7.5 to 12.6 wt.% (Figure 7). This behavior can be explained by two opposing effects. At low monomer concentrations, increasing molecular weight of PGMA graft chains in PGMA-*graft*-PAA copolymer accelerated adsorption of stabilizer improving thus the stabilization efficiency. This resulted in greater number of smaller particles [37,39]. On the contrary, at high GMA concentrations ( $\sim 7.5$  wt.% and more), effect of better solubility of PGMA in reaction medium, and as a consequence precipitation of oligomer chains at longer critical chain length, prevailed the influence of the stabilizer. Therefore, the PGMA microsphere size increased with growing GMA concentration [16,39].

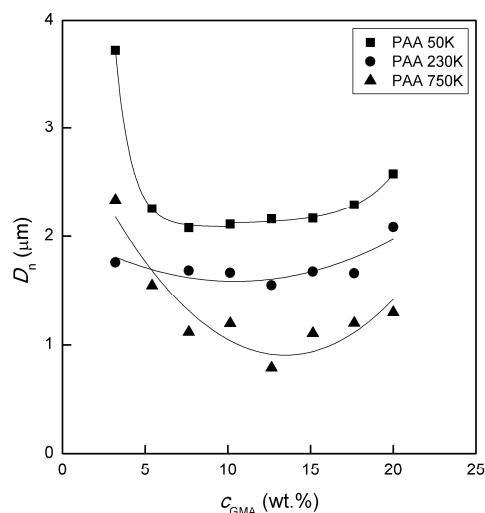


**Figure 7.** Dependence of PGMA microsphere diameter  $D_n$  on the concentration of GMA in EtOH.

### Effect initiator concentration

In dispersion polymerization of GMA, AIBN was chosen as a suitable initiator due to its good solubility in alcoholic media and ability to produce regular and monodisperse particles. The PGMA microsphere size increased with increasing AIBN concentration (Figure 8), which could be due to the higher concentration of free radicals ensuring higher concentration of polymer chains in the reaction mixture [16]. However, more polymer chains of lower molecular weight were formed and as fewer PGMA chains reached the critical size, fewer nucleation sites were available. Capture of the oligomer chains from the continuous phase and enhanced aggregation process then contributed to the formation of larger microspheres [16,37].

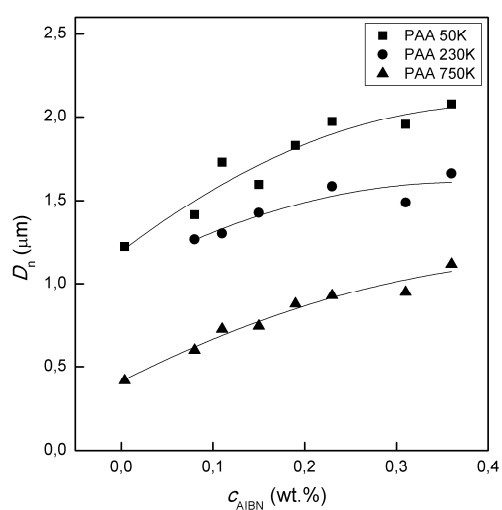


**Figure 8.** Dependence of PGMA microsphere diameter  $D_n$  on the concentration of AIBN in EtOH.

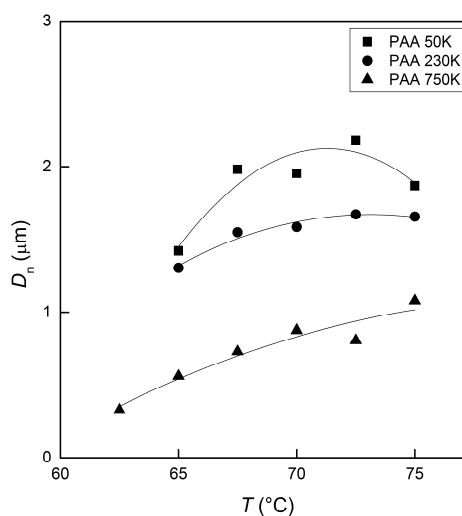


**Figure 9.** Dependence of the PGMA microsphere diameter  $D_n$  on the polymerization temperature.

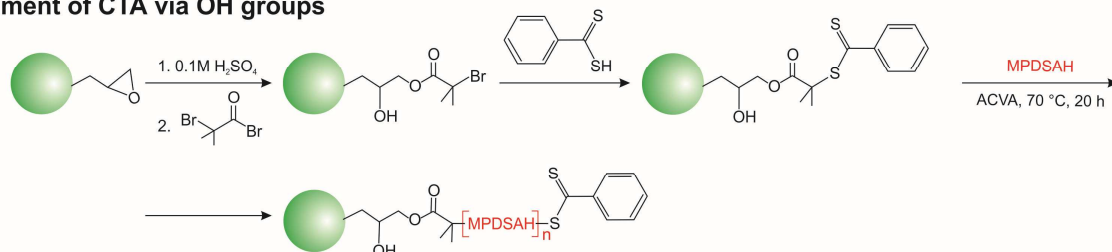
### Effect of polymerization temperature

The reaction temperature has to be sufficiently high to ensure high radical concentration during the polymerization process; however, the medium must not evaporate. The increase in the temperature led to the formation of larger PGMA microspheres (Figure 9), which can be ascribed to several factors. First, due to increased solubility of PGMA chains at higher polymerization temperatures, the critical chain length was extended. Moreover, with increasing temperature, both the initiator decomposition rate and propagation rate were higher. As a result, more free radicals were formed during the same period of time and particle growth was enhanced. Last but not least, the stabilizer adsorption was reduced at higher temperatures due to the increased solubility of PAA in EtOH [16]. All these factors together with lower medium viscosity contributed to increase in the PGMA microsphere size.

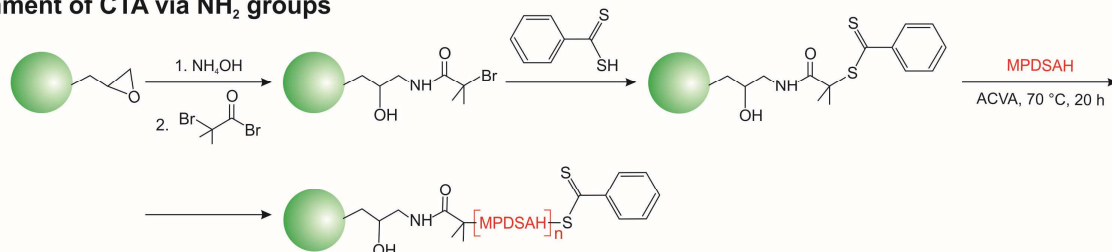
## 5.2 Attachment of dithiobenzoic acid to the particle surface

The main advantage of PGMA microspheres prepared by polymerization in EtOH is the high content of oxirane reactive groups (90–95 wt.%). The initial PGMA microspheres were 2.2  $\mu\text{m}$  in size, with  $PDI = 1.02$ , and contained 5.5 mmol of oxirane groups/g. The surface-initiated RAFT polymerization can be realized via a surface-anchored initiator or a chain transfer agent (CTA). In this work, surface-immobilized CTA was chosen due to relatively mild reaction conditions. From various CTAs, dithiobenzoates are recommended RAFT agents for polymerization of methacrylamide-based monomers [25].

### a) Attachment of CTA via OH groups



### b) Attachment of CTA via $\text{NH}_2$ groups



### c) Attachment of CTA via oxirane groups

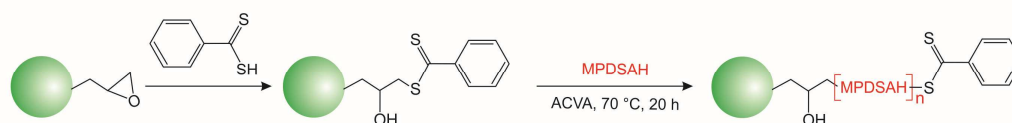


**Figure 10.** Scheme of DTBA attachment to the PGMA microspheres via hydroxyl or amino groups and BIBB initiator (a, b) and via direct opening of oxirane groups (c).

Based on the recommendation, dithiobenzoic acid (DTBA) was chosen as the CTA for polymerization of zwitterionic meth-acrylamide. The DTBA transfer agent can be bound to the PGMA microspheres via several approaches including direct opening of oxirane groups or attachment via ATRP initiator (Figure 10). The main advantage of DTBA is its relatively easy synthesis and mild reaction conditions during the immobilization process, however, it is susceptible to light- and oxygen-induced reactions and, therefore, it needs to be consumed immediately after its synthesis [40].

### Attachment of $\alpha$ -bromoisobutyryl bromide

Prior to  $\alpha$ -bromoisobutyryl bromide (BIBB) attachment, the oxirane groups of PGMA microspheres were either hydrolyzed in diluted sulfuric acid yielding poly(2,3-dihydroxypropyl methacrylate) (PDHPMA), or ammonolyzed in 25% aqueous ammonia to obtain poly(2-hydroxy-3-aminopropyl methacrylate) (PHAPMA) [41]. The morphology, size, *PDI* and dispersibility in water of both PDHPMA and PHAPMA microspheres were preserved. Theoretically, the PDHPMA microspheres contained 10 mmol OH/g, PHAPMA microspheres *ca.* 1.9 mmol NH<sub>2</sub>/g. The ATRP initiators possess in the structure C–X bond that can be used for attachment of RAFT agent. In order to find optimum amount of the particle-bound initiator, several BIBB/OH molar ratios (0.1–1.1 mol/mol) were examined. The PDHPMA-BIBB microspheres with attached initiator contained 3–67 wt.% BIBB (Figure 11). In order to avoid the growth of polymer chains from deep inside of the particles, PDHPMA-BIBB microspheres with lower BIBB content ( $\leq 30$  wt.%) were preferred because in this case the BIBB was supposed to be localized predominantly on the particle surface [42].

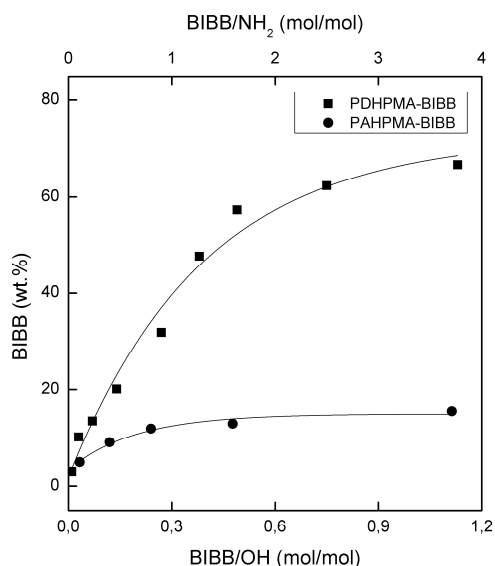


**Figure 11.** Dependence of PDHPMA- and PHAPMA-BIBB on BIBB/OH and BIBB/NH<sub>2</sub> molar ratio in reaction mixture.

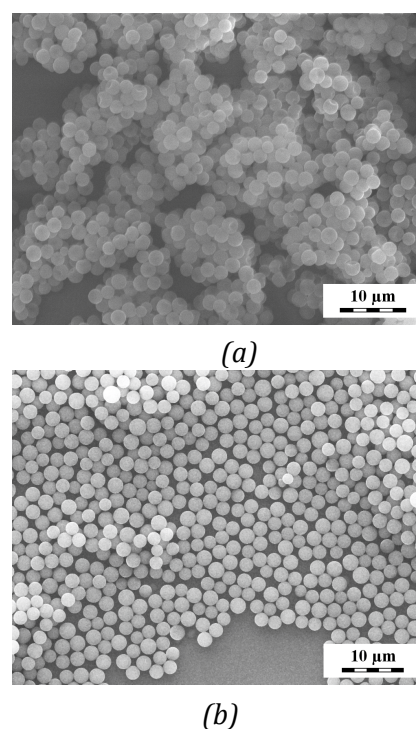


**Figure 12.** SEM micrographs of PDHPMA-BIBB (a; 9.2 wt.% BIBB) and PHAPMA-BIBB microspheres (b; 8.8 wt. % BIBB).

Amount of the BIBB attached to the PHAPMA microspheres was significantly lower than in the PDHPMA-BIBB microspheres (Figure 11). At 0.2–3.7 BIBB/NH<sub>2</sub> molar ratios, content of the BIBB in PHAPMA-BIBB microspheres reached only 5–16 wt.%. The reason of rather low BIBB content could consist in a lower concentration of amino groups that react with BIBB preferentially to hydroxyls. After attachment of BIBB via the amino groups, BIBB does not react with hydroxyl groups mainly due to the steric barrier. Size of the PDHPMA-BIBB with lower BIBB content ( $\leq 30$  wt.%) and PHAPMA-BIBB microspheres was preserved (Figure 12).

### Attachment of dithiobenzoic acid

DTBA was attached to the PGMA particles via three different approaches (Figure 10). The easiest way requiring no previous particle activation consisted in the direct reaction of oxirane groups with the DTBA yielding PGMA-DTBA microspheres. During the experiments, several DTBA/oxirane groups ratios (0.2–2.2 mol/mol) were tested; amount of the surface-attached DTBA reached from 0.05 to 4.7 wt.% (Figure 13 a). The main drawback of this approach lied in an extensive particle aggregation caused by their swelling in the reaction medium and subsequent flocculation during the DTBA immobilization (Figure 14 a).

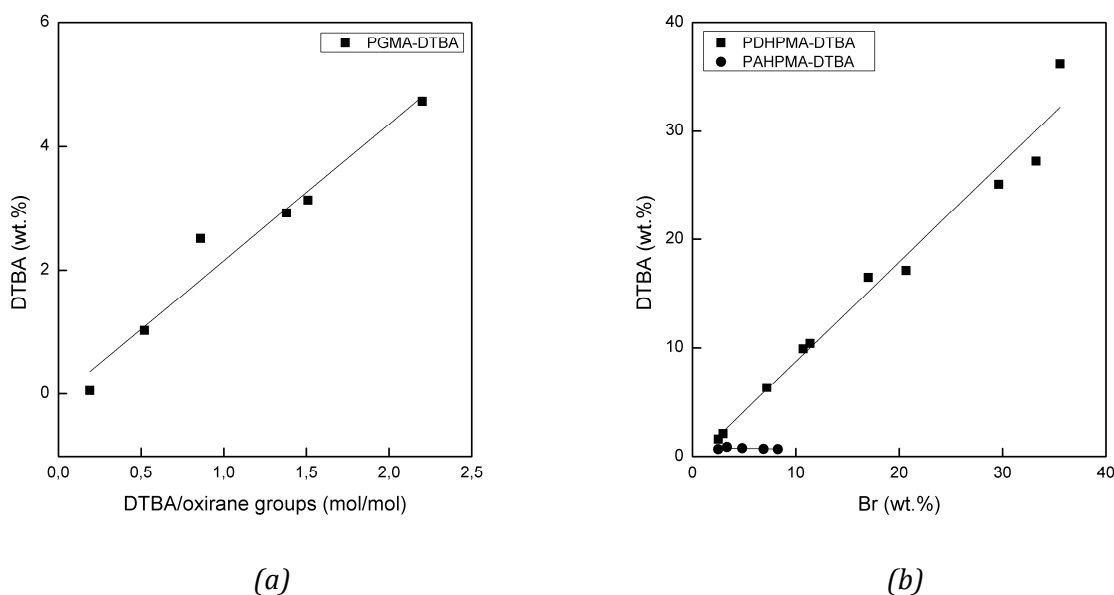


**Figure 13.** Dependence of amount of DTBA attached to PGMA microspheres at various DTBA/oxirane group ratios (a) and of amount of DTBA attached to PDHPMA-DTBA and PHAPMA-DTBA microspheres containing different amount of Br (b).

DTBA was bound to the PDHPMA-BIBB and PHAPMA-BIBB microspheres containing different amount of BIBB, which resulted in PDHPMA-DTBA and PHAPMA-DTBA microspheres, respectively. The DTBA/Br ratio was kept constant at 1:1 mol/mol. Amount of the DTBA in the PDHPMA-DTBA microspheres increased linearly with increasing Br content reaching up to 36 wt.% DTBA (Figure 13 b). This was probably a consequence of higher C–Br bond reactivity compared with that of initial oxirane groups. Amount of DTBA attached to the PHAPMA-BIBB particles was almost constant ( $< 0.9$  wt.%) and independent on the amount of

BIBB in the microspheres (Figure 13 b). The reason of this behavior could be rather low amount of BIBB in the PHAPMA-BIBB compared with its content in the PDHPMA-BIBB microspheres, degradation of DTBA caused by unreacted amino groups and also cyclization of attached BIBB with free hydroxyl groups. Under certain conditions, hydroxyl groups can react with alkylhalogenides forming thus ether bonds [43]. All these factors could lead to small DTBA content in the PHAPMA-DTBA microspheres. However, morphology, size and *PDI* of both the PDHPMA-DTBA and the PHAPMA-DTBA microspheres were preserved (Figure 14 b, c).

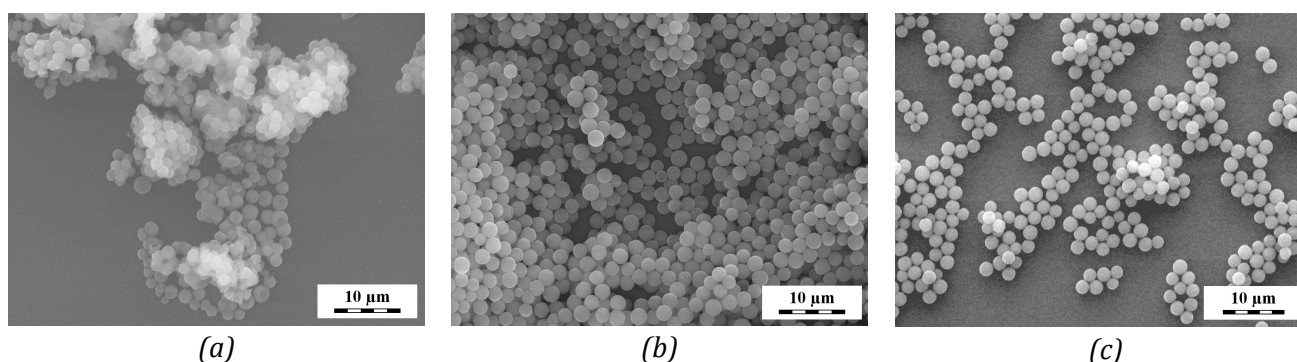


**Figure 14.** SEM micrographs of PGMA-DTBA (a), PDHPMA-DTBA (b) and PAHPMA-DTBA microspheres (c).

### 5.3 Surface-initiated RAFT polymerization

As a monomer used for surface modification of the PGMA microspheres, zwitterion [3-methacryloylamino)propyl]-dimethyl(3-sulfopropyl)ammonium hydroxide (MPD<sub>SAH</sub>; Figure 15) was chosen mainly due to its resistance to nonspecific protein adsorption [34,44]. In comparison with other zwitterions, MPD<sub>SAH</sub> has a minimum tendency to hydrolysis, is stable in aqueous media even at higher temperatures and can be easily synthesized [45,46]. Moreover, the presence of amide bond increases a hydration of poly{[3-methacryloylamino)-propyl]dimethyl(3-sulfopropyl)ammonium hydroxide} (PMPD<sub>SAH</sub>) chains and prevents thus fouling of protein molecules [34].

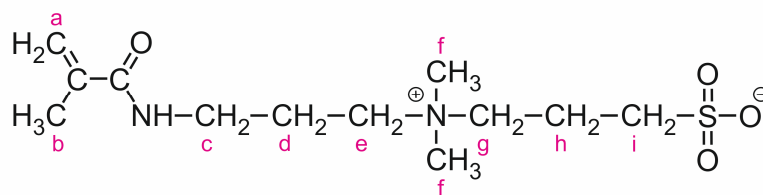


**Figure 15.** Structure of MPD<sub>SAH</sub> monomer.

First, polymerization of MPD<sub>SAH</sub> was carried out from the PGMA-DTBA microspheres in various solvents (water, acetic buffer, MeOH, EtOH) with ACVA as an initiator. Except for the polymerization in MeOH and EtOH, amount of the grafted PMPD<sub>SAH</sub> (calculated from the nitrogen content) was very low (0.8–1.5 wt.%) and independent on the reaction conditions, i.e. on the amount of surface-attached DTBA, DTBA/ACVA molar ratio and reaction medium composition. Amount of the PMPD<sub>SAH</sub> grafted from microspheres in EtOH and MeOH was significantly higher (~ 3 wt.% in EtOH and 21 wt. % in MeOH).

Increase in the PMPDSAHA content could be explained by poorer solubility of PMPDSAHA chains in EtOH and MeOH than in aqueous media, which increased presence of the PMPDSAHA close to the particle surface and supported growth of PMPDSAHA from the surface [46,47]. However, the extensive aggregation of the PGMA-DTBA microspheres disabled them from applications in real biological experiments even after their surface modification. Therefore, PDHPMA-DTBA microspheres with the DTBA attached via BIBB initiator were preferred to the PGMA-DTBA microspheres mainly due to the preserved morphology, size, *PDI* and dispersibility in aqueous media. Moreover, fragmentation rate of the  $\cdot\text{C}(\text{CH}_3)_2\text{COOR}$  radical in the PDHPMA-DTBA is significantly higher than that of the  $\cdot\text{CH}_2\text{R}$  in the PGMA-DTBA microspheres, which should ensure better control of the RAFT polymerization [25].

Polymerization of MPDSAHA on the PDHPMA-DTBA microspheres was carried out in water at a constant monomer concentration and various DTBA/ACVA ratios. Even though, morphology of the PDHPMA-PMPDSAHA microspheres remained unchanged (Figure 17 a), amount of the grafted PMPDSAHA reached only 1.2–1.9 wt.% (Table 1). Analogously, the polymerization in acetic buffer (pH 5.2) with various MPDSAHA contents (0.4–1.2 g) and at constant DTBA/ACVA molar ratio did not lead to increase in the PMPDSAHA content on the PDHPMA-PMPDSAHA microspheres (Table 1).

**Table 1.** RAFT polymerization from PDHPMA-DTBA and properties of PDHPMA-PMPDSAHA microspheres.

DTBA/ACVA (mol/mol)	Polymerization medium	$C_{\text{MPDSAHA}}^a$ (g)	$S_{\text{before}}^b$ (wt.%)	$S_{\text{after}}^c$ (wt.%)	N (wt.%)	PMPDSAHA (wt.%)	$D_n^d$ (μm)	<i>PDI</i> <sup>e</sup>
16*	Water	0.4	4.35	4.55	0.18	1.88	2.3	1.02
32*		0.4		4.06	0.11	1.15	2.3	1.02
12**	Acetic buffer	0.4	1.35	0.86	0.06	0.63	2.2	1.03
12**		0.8		1.03	0.07	0.73	2.2	1.03
12**		1.2		1.01	0.09	0.94	2.2	1.03

\* 680 μmol DTBA/g particles; \*\* 211 μmol DTBA/g particles; <sup>a</sup> amount of MPDSAHA in the polymerization feed; <sup>b</sup> content of sulfur on the PDHPMA-DTBA microspheres before the polymerization; <sup>c</sup> content of sulfur on PDHPMA-PMPDSAHA microspheres after the RAFT polymerization; <sup>d</sup> number-average diameter; <sup>e</sup> index of polydispersity.

In order to increase amount of the grafted PMPDSAHA, the polymerization of the MPDSAHA was performed in polar organic solvents (MeOH, EtOH and DMF/acetic buffer). Unlike the polymerization in aqueous media, amount of the PMPDSAHA grafted on the PDHPMA-DTBA microspheres in MeOH and EtOH significantly increased up to 2–14 wt.% (Table 2). Moreover, content of the PMPDSAHA grew with increasing amount of the monomer in the reaction feed. This increase could prove successful polymerization and growing molecular weight of the grafted polymer [25]. On the other hand, polymerization of the MPDSAHA in DMF/acetic buffer did not improve PMPDSAHA yield due to the aminolysis of DTBA during the reaction. Therefore, DMF was found to be a poor medium for polymerization of the MPDSAHA.

Since concentration of the CTA determines extent of the chain transfer reactions, its concentration has also an impact on the molecular weight and the amount of the grafted polymer chains [47,48]. During the experiments, PDHPMA-DTBA microspheres containing

437 (Table 2), 1,140 and 134  $\mu\text{mol}$  DTBA/g were investigated (Table 3). Amount of the PMPDSAHA grafted on all PDHPMA-DTBA microspheres increased with higher concentration of MPDSAHA in the polymerization feed and reached 6.2 –12 wt.% on microspheres with 1,140  $\mu\text{mol}$  DTBA/g and up to 20 wt.% on microspheres containing 134  $\mu\text{mol}$  DTBA/g. This is in agreement with previously published results, when higher concentrations of CTA led to retardation of the RAFT polymerization and, thus, to a lower amount of the grafted polymer chains [48,49]. The retardation was explained by a relatively high local CTA concentration that is very often one order of magnitude higher than that in the solution polymerization. Due to the high CTA concentration, the free radicals formed on a solid surface upon CTA fragmentation have no tendency to propagate with the monomer, but they transfer between neighboring CTA molecules. This degenerative transfer then causes the retardation and even inhibition of the RAFT process [48,49]. Size of the zwitterion-modified microspheres increased from 2.2 up to 2.6  $\mu\text{m}$  depending on amount of the grafted PMPDSAHA; the index of polydispersity did not change (Figure 16 b, c).

**Table 2.** Influence of reaction medium and monomer concentration on amount of the PMPDSAHA grafted from PDHPMA-DTBA microspheres containing 437  $\mu\text{mol}$  DTBA/g.

Polymerization media	$C_{\text{MPDSAHA}}^{\text{a}}$ (g)	$S_{\text{before}}^{\text{b}}$ (wt.%)	$S_{\text{after}}^{\text{c}}$ (wt.%)	N (wt.%)	PMPDSAHA (wt.%)	$D_n^{\text{d}}$ ( $\mu\text{m}$ )	$PDI^{\text{e}}$
MeOH	0.4	2.80	2.83	0.18	1.88	2.2	1.02
	0.8		3.05	0.59	6.16	2.2	1.02
	1.2		3.13	0.79	8.25	2.3	1.03
EtOH	0.4		3.23	0.77	8.04	2.3	1.03
	0.8		5.62	1.33	13.89	2.3	1.03
	1.2		4.28	1.08	11.28	2.3	1.03

<sup>a</sup> Amount of MPDSAHA in the polymerization feed; DTBA/ACVA = 24 mol/mol; <sup>b</sup> content of sulfur in PDHPMA-DTBA microspheres before the polymerization; <sup>c</sup> content of sulfur in PDHPMA-MPDSAHA microspheres after the RAFT polymerization; <sup>d</sup> number-average diameter; <sup>e</sup> index of polydispersity.

**Table 3.** Influence of DTBA and monomer concentration on amount of the PMPDSAHA grafted in MeOH from PDHPMA-DTBA microspheres containing different amounts of DTBA.

$C_{\text{DTBA}}$ ( $\mu\text{mol/g}$ )	$C_{\text{MPDSAHA}}^{\text{a}}$ (g)	$S_{\text{before}}^{\text{b}}$ (wt.%)	$S_{\text{after}}^{\text{c}}$ (wt.%)	N (wt.%)	PMPDSAHA (wt.%)	$D_n^{\text{d}}$ ( $\mu\text{m}$ )	$PDI^{\text{e}}$
1,140*	0.4	7.30	6.98	0.78	8.15	2.3	1.02
	0.8		7.07	1.14	11.90	2.4	1.02
	1.2		6.61	0.60	6.27	2.3	1.02
134**	0.4	0.87	1.54	0.27	2.82	2.2	1.02
	0.8		2.24	1.31	13.68	2.5	1.04
	1.2		2.88	1.90	19.84	2.6	1.06

\* DTBA/ACVA = 24 and \*\* 7.5 mol/mol; <sup>a</sup> amount of MPDSAHA in the polymerization feed; <sup>b</sup> content of sulfur in PDHPMA-DTBA microspheres before the RAFT polymerization; <sup>c</sup> content of sulfur in PDHPMA-MPDSAHA microspheres after the RAFT polymerization; <sup>d</sup> number-average diameter; <sup>e</sup> index of polydispersity.

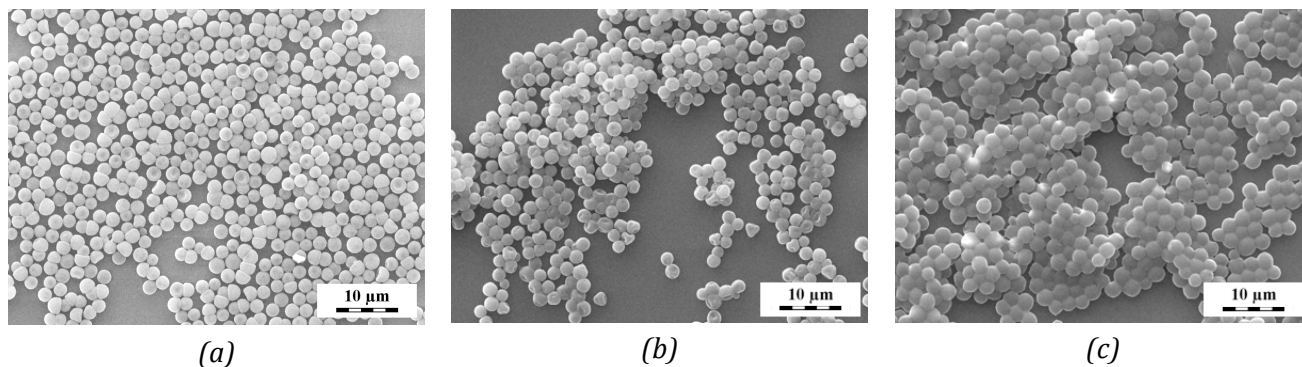


**Figure 16.** SEM micrographs of PDHPMA-PMPDSAHA microspheres prepared in water (a) and MeOH (b, c) and containing 1.2 (a), 6.2 (b) and 13.7 wt.% PMPDSAHA (c). The DTBA content before RAFT polymerization was 680 (a), 437 (b) and 134  $\mu\text{mol/g}$  (c).

#### 5.4 Characterization of RAFT polymerization of MPDSAHA

In order to find mechanism of RAFT polymerization of the MPDSAHA, decrease and increase of the monomer and polymer concentration, respectively, during the polymerization was studied by size exclusion chromatography. Retention times of monomer, oligomer and polymer were measured and their peak areas in the chromatograms compared.

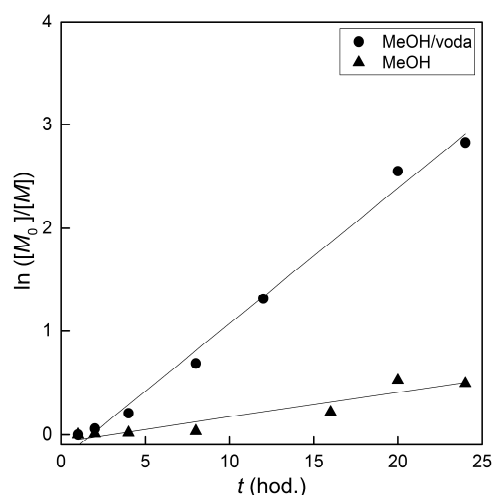


**Figure 17.** Dependence of the  $\ln([M_0]/[M])$  ratio on the polymerization time in MeOH/H<sub>2</sub>O and MeOH.

In the typical RAFT polymerization, the dependence of the logarithm of initial to instant monomer concentration ratio  $\ln([M_0]/[M])$  should be linear [25]. The dependence of  $\ln([M_0]/[M])$  on the polymerization time in MeOH/H<sub>2</sub>O mixture was linear (Figure 17) showing relatively quick MPDSAHA consumption, as well as the PMPDSAHA formation; 50 % of PMPDSAHA was present after 8 h of the reaction. On the contrary, the  $\ln([M_0]/[M])$  ratio in neat MeOH slightly differed from the linear behavior (Figure 17) and the polymerization was significantly retarded as the polymer peak was detected until after 16 h. Explanation of the deviation could be the different amount of PMPDSAHA on the PDHPMA microspheres in both MeOH/H<sub>2</sub>O and MeOH media (~ 3 wt.% in MeOH/H<sub>2</sub>O and 6–17 wt.% in MeOH). Thus, detection of the solution PMPDSAHA in MeOH was more misrepresented than in the MeOH/H<sub>2</sub>O

mixture. Another reason of the nonlinear behavior could consist in slow initiation of the polymerization of MPD<sub>2</sub>SAH in MeOH. Though, the polymerization in the MeOH/H<sub>2</sub>O mixture showed relatively fast monomer consumption and polymer formation, microspheres with grafted PMPD<sub>2</sub>SAH were not synthesized. This was ascribed to better solubility of PMPD<sub>2</sub>SAH in the polymerization media, and thus, to tendency of polymer chains to remain in solution instead on the particle surface.

## 5.5 Characterization of surface-modified PDHPMA microspheres

### *Infrared spectroscopy*

As the original ATR FTIR spectra of starting and modified PDHPMA microspheres demonstrated minimal changes, only the differential spectra are shown (Figure 18). Band with a maximum at  $\sim 3,475$   $\text{cm}^{-1}$  and peaks with maxima at about 1,272 and 1,148  $\text{cm}^{-1}$  increased in differential spectrum of PDHPMA-BIBB minus PDHPMA (Figure 18, spectrum 1). The first was ascribed to stretching vibrations of OH groups, the latter to vibration of C–O and C–OH bonds after attachment of BIBB [50]. After binding of DTBA to the PDHPMA-BIBB microspheres, sharp peak at 1,044  $\text{cm}^{-1}$  corresponding to C(=S)S vibrations appeared in the original ATR FTIR spectra [51]. In the differential spectrum, increase of the broad band with maximum at  $\sim 3,475$   $\text{cm}^{-1}$  was related to the vibration of OH groups (Figure 18, spectrum 2). The newly formed peaks at about 1,089 and 1,048  $\text{cm}^{-1}$  were ascribed to skeletal C–C vibrations of the aromatic ring and C(=S)S vibrations of the thiocarbonyl group of DTBA, respectively [50,51].

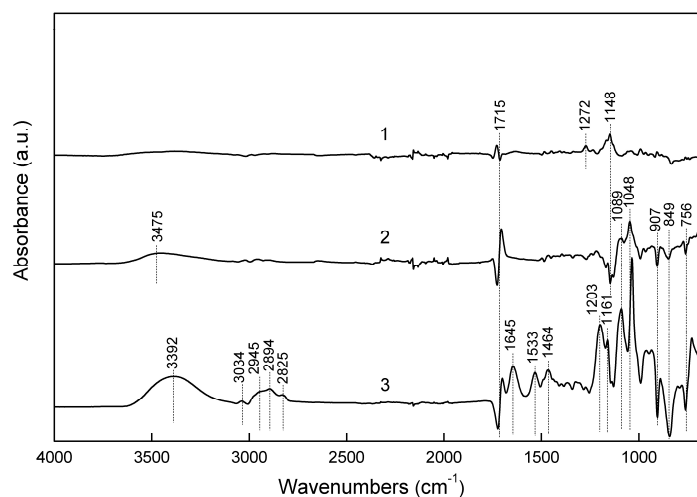


**Figure 18.** Differential ATR FTIR spectra of PDHPMA-BIBB minus PDHPMA (1), PDHPMA-DTBA minus PDHPMA-BIBB (2) and PDHPMA-PMPD<sub>2</sub>SAH minus PDHPMA-DTBA (3).

After surface modification with PMPD<sub>2</sub>SAH, two new peaks at 1,645 and 1,533  $\text{cm}^{-1}$  appeared in the differential spectrum (Figure 18, spectrum 3). These two peaks corresponded to the C=O (amide I) and N–H (amide II) vibrations [51]. Presence of amide bond originated

from MPDSAHA zwitterion was also confirmed by broad band with maximum  $\sim 3,392\text{ cm}^{-1}$  belonging to the N–H stretching vibration [51]. Increased number of  $\text{CH}_2$  groups was reflected in the bands with maxima at about  $3,034\text{--}2,883\text{ cm}^{-1}$  [50]. Positive peak at  $1,464\text{ cm}^{-1}$  corresponded to vibration of quaternary ammonium groups originated from PMPDSAHA chains [44,50]. Broad band at  $1,048\text{ cm}^{-1}$  belonged to the stretching vibration of sulfonate groups, however, it could be partly overlapped by vibration of thiocarbonyl groups of DTBA [50].

### Zeta potential

The resistance to nonspecific protein adsorption is influenced by electrostatic interactions of the material and the proteins. Therefore, it is important to know the surface charge of the proteins and that of the studied substrate. The surface charge of polymer microspheres can be expressed by the  $\xi$  potential.

Zeta potential of the initial and the surface-modified PGMA microspheres was determined in phosphate buffer (PBS; pH 7.3). Absolute value of  $\xi$  potential of the initial PGMA microspheres decreased from *ca.* 31 mV to *ca.* 18 mV after attachment of the hydrophobic DTBA and up to *ca.* 15 mV after the PMPDSAHA grafting. Moreover, absolute value of the  $\xi$  potential further decreased to *ca.* 10 mV with increasing amount of grafted PMPDSAHA.

In theory, polyzwitterions should have neutral charge at pH 7 due to the presence of both positive and negative charge on each monomer unit [31,34,52]. However, neutral charge of PDHPMA-PMPDSAHA particles was not observed. Therefore, dependence of  $\xi$  potential on the pH and ionic strength of NaCl solution was measured (Figure 19). The  $\xi$  potential of the initial PGMA microspheres decreased in the whole pH range; the decrease in the solution of low ionic strength was more pronounced (Figure 19 a, b). The PGMA microspheres were stabilized with PAA and therefore, their negative surface charge was ascribed to deprotonation of carboxyl groups of the PAA [52].

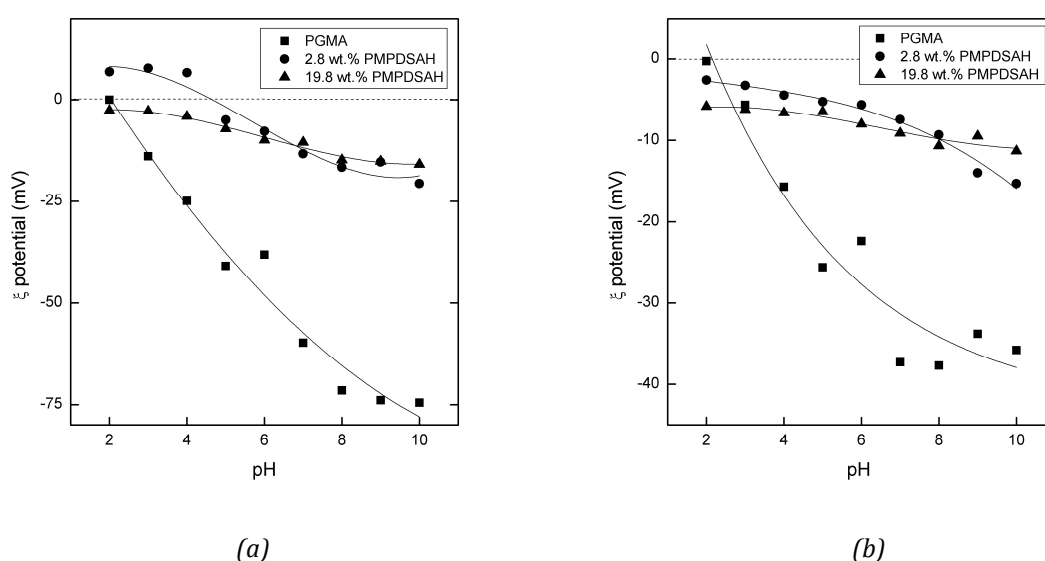


**Figure 19.** Dependence of  $\xi$  potential on the pH of dispersion containing initial PGMA and PDHPMA-PMPDSAHA microspheres modified with low and high amount of PMPDSAHA in 0.01M (a) and 0.1M NaCl solution (b).

Dependence of  $\xi$  potential of PDHPMA-PMPDSAHA microspheres with low amount of grafted PMPDSAHA (~ 3 wt.%) was changed from the positive to the negative charge (Figure 19 a). While in acidic solutions the positively charged ammonium ions were activated, negatively charged sulfonic groups were deprotonated in basic solutions. On the other hand, PDHPMA-PMPDSAHA microspheres containing high amount of PMPDSAHA (~ 20 wt.%) were negatively charged over pH range 2–10 (Figure 19 a). This phenomenon could be explained by presence of strongly acidic sulfonate groups on the particle surface. In general, the net charge is determined by the acid-base equilibrium involving the sulfonate and tetraalkylammonium groups. Strong acidity of the sulfonate groups caused that almost all were in the form of anions. Besides, some tetraalkylammonium ions associated with the OH<sup>-</sup> ions in solution and formed uncharged tetraalkylammonium hydroxide [53]. Because the negatively charged sulfonate ions prevailed the positively charged ammonium groups, the PMPDSAHA, and consequently PMPDSAHA-covered microspheres, had an overall negative charge [53]. To reach charge neutrality of the polymer, pH would have to be shifted in favor of positively charged tetraalkylammonium ions [53]. Due to the reduced concentration of sulfonate groups on the PDHPMA-PMPDSAHA microspheres with low amount of PMPDSAHA, the acid-base equilibrium, i.e., the overall neutral charge was reached at higher pH than on microspheres with high PMPDSAHA content.

The overall negative charge of both types of PDHPMA-PMPDSAHA microspheres within the whole pH range was observed also in 0.1M NaCl solution (Figure 19 b). Decrease of absolute value of the  $\xi$  potential was ascribed to partial compensation of the overall negative charge of the PDHPMA-PMPDSAHA microspheres caused by preferential interactions of negatively charged sulfonate groups with counter ions in the solution [54].

## 5.6 Nonspecific protein adsorption on microspheres

Resistance of PDHPMA-PMPDSAHA microspheres to nonspecific adsorption was tested in PBS buffer (pH 7.3) using bovine serum albumin (BSA) as a model protein. Initial PGMA microspheres showed very low BSA adsorption ~ 4 wt.% of original BSA amount in the solution. Resistance of the starting microspheres could be induced by presence of the hydrophilic carboxyl groups originated from the PAA stabilizer. Moreover, oxirane groups in the initial PGMA microspheres could be hydrolyzed, producing vicinal hydroxyl groups. Both these groups could participate in creation of hydration water layer preventing thus contacts of BSA with the particle surface [53]. Both PGMA microspheres and BSA protein had negative  $\xi$  potential in PBS buffer (*ca.* -31 and -28 mV, respectively) and, thus, repulsive electrostatic interactions could increase resistance of the PGMA microspheres to nonspecific adsorption [55]. After attachment of DTBA, adsorption of the BSA on PDHPMA-DTBA microspheres doubled (Figure 20). This behavior was ascribed to hydrophobization of the particle surface by DTBA. Any hydrophobic surface hinders formation of the hydration water layer and causes protein denaturation, associated with loss of protein conformation and, as a consequence, increases protein adsorption [56].

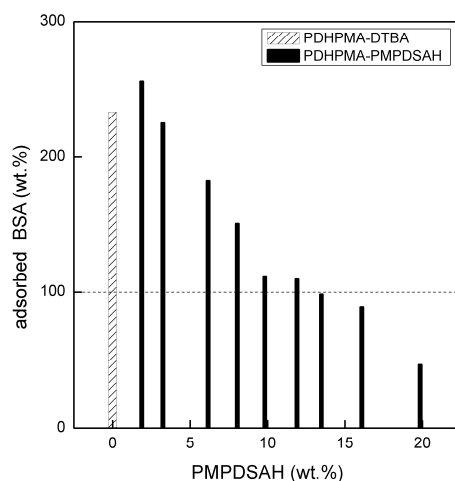


**Figure 20.** Amount of BSA adsorbed on PDHPMA-PMPDSAHA microspheres. Amount of the BSA is related to its amount captured on the initial PGMA microspheres.

Nonspecific BSA adsorption increased after modification of the PDHPMA microspheres with PMPDSAHA, however with growing amount of PMPDSAHA the adsorption gradually decreased up to 47 wt.% of BSA amount adsorbed on the initial PGMA microspheres (Figure 20). With higher amount of PMPDSAHA grafted on the microspheres, absolute value of the  $\xi$  potential decreased towards zero. Thus, a decrease in the electrostatic repulsion leading to increased protein adsorption could be assumed [57]. However, electrostatic interactions play an important role mainly in solutions of low ionic strength and they decrease at their higher values [57,58]. Thus, the factor determining resistance to the nonspecific protein adsorption is ability of the surface to form the hydration water layer that excludes protein molecules from the surface surroundings [34]. Sufficient concentration of ammonium and sulfonate groups originating from the microspheres containing > 13 wt.% of PMPDSAHA resulted in good surface hydration of the PDHPMA-PMPDSAHA microspheres and prevented thus the protein denaturation and contacts of BSA with particle surface [58].

## 6. CONCLUSIONS

In the thesis, preparation of new polymer microspheres and their surface modification with the aim to reduce nonspecific protein adsorption is presented. At first, PGMA microspheres with the size ranging from 0.5–5.4  $\mu\text{m}$  were prepared by the dispersion polymerization in EtOH using PAA as a stabilizer. The particle size was strongly influenced by polarity of the reaction mixture and type of the co-solvent. Predominantly, increasing amount of water in the mixture (i.e., increasing solubility parameter) caused significant increase in the particle size (more than by 3.4  $\mu\text{m}$ ). The particle size distribution was strongly affected by the molecular weight of the PAA stabilizer. Whereas both PAAs ( $M_w = 50,000$  and

230,000) allowed formation of the PGMA microspheres with  $PDI < 1.1$ , monodisperse particles stabilized with high-molecular-weight PAA ( $M_w = 750,000$ ) were not obtained under any reaction conditions.

The PGMA microspheres, 2.2  $\mu\text{m}$  in size, stabilized with PAA of  $M_w = 50,000$  were used for subsequent surface modification. In order to perform surface-initiated RAFT polymerization, the microsphere surface was functionalized with chain transfer agent. Dithiobenzoic acid was covalently attached to the microspheres using three different approaches: direct reaction of DTBA with oxirane groups of PGMA and attachment of ATRP initiator via amino or hydroxyl groups of PHAPMA or PDHPMA microspheres. Both the direct reaction and the activation with ATRP initiator via amino groups were discontinued since the first approach caused extensive particle aggregation and the second method produced minimal amount of DTBA bound to the microspheres. Only hydrolysis of the PGMA microspheres, attachment of the ATRP initiator and, subsequently, of CTA allowed introduction of the dithiobenzoate functional groups (up to 36 wt.%). At the same time, particle size, morphology,  $PDI$  and dispersibility in aqueous media were preserved.

Surface-initiated RAFT polymerization of MPD<sub>2</sub>SAH zwitterion was carried out on microspheres containing  $< 1.2$  mmol DTBA/g first in aqueous media, later on in polar organic solvents. Only the polymerization in MeOH and EtOH allowed to graft PMPD<sub>2</sub>SAH from the particle surface. This behavior was ascribed to limited solubility of the polymer in the reaction medium and thus, to tendency of the polymer to remain close to the surface. Besides, with the increasing monomer concentration, microspheres containing different amount of the PMPD<sub>2</sub>SAH were prepared. The successful modification was confirmed by infrared spectroscopy and by change of  $\zeta$  potential. Absolute value of the  $\zeta$  potential decreased with increasing amount of PMPD<sub>2</sub>SAH on the microspheres. Whereas the  $\zeta$  potential of the microspheres containing low amount of the PMPD<sub>2</sub>SAH was changed from positive to negative value, microspheres modified with high amount of PMPD<sub>2</sub>SAH showed only negative  $\zeta$  potential within the whole pH range. This was ascribed to presence of the dissociated sulfonate groups and partial neutralization of tetraalkylammonium groups of the PMPD<sub>2</sub>SAH chains.

Last but not least, resistance of the PMPD<sub>2</sub>SAH-modified microspheres to nonspecific adsorption was verified using BSA as a model protein. The nonspecific interactions decreased with higher amount of PMPD<sub>2</sub>SAH, up to one half of that on the initial microspheres. This decrease was most probably ensured by good hydration of the particle surface, and thus, by hindering the protein-surface interactions.

## 7. LIST OF ABBREVIATIONS

ACVA	4,4'-Azobis(4-cyanopentanoic acid)
AIBN	2,2'-Azobis(2-methylpropanionitrile)
ATR-FTIR	Fourier transform infrared spectroscopy with attenuated total reflectance
ATRP	Atom transfer radical polymerization

BIBB	$\alpha$ -Bromoisobutyryl bromide
BSA	Bovine serum albumin
<i>c</i>	Concentration (wt.%)
CMC	Critical micellar concentration
CTA	Chain transfer agent
$D_n$	Number-average diameter ( $\mu\text{m}$ )
$D_w$	Weight-average diameter ( $\mu\text{m}$ )
DMF	<i>N,N</i> -Dimethylformamide
DTBA	Dithiobenzoic acid
EtCel	2-Ethoxyethanol
EtOH	Ethanol
GMA	Glycidyl methacrylate
$[M_0]$ , $[M]$	Initial and instant monomer concentration (%)
MeOH	Methanol
MPDSAH	[3-(Methacryloylamino)propyl]-dimethyl(3-sulfopropyl)ammonium hydroxide
NMP	Nitroxide mediated polymerization
PAA	Poly(acrylic acid)
PBS	Phosphate buffer saline
PDHPMA	Poly(2,3-dihydroxypropyl methacrylate)
PDHPMA-BIBB	Poly(2,3-dihydroxypropyl methacrylate) microspheres with attached $\alpha$ -bromo-isobutyryl bromide
PDHPMA-DTBA	Poly(2,3-dihydroxypropyl methacrylate) microspheres with attached dithiobenzoic acid
PDHPMA-PMPDSAH	poly(2,3-dihydroxypropyl methacrylate) microspheres with grafted poly{[3-methacryloylamino)propyl]-dimethyl(3-sulfopropyl)ammonium hydroxide}
<i>PDI</i>	Index of polydispersity
PEG	Poly(ethylene glycol)
PGMA	Poly(glycidyl methacrylate)
PGMA-DTBA	Poly(glycidyl methacrylate) microspheres with attached dithiobenzoic acid
PHAPMA	Poly(2-hydroxy-3-aminopropyl methacrylate)
PHAPMA-BIBB	Poly(2-hydroxy-3-aminopropyl methacrylate) microspheres with attached $\alpha$ -bromoisobutyryl bromide
PHAPMA-DTBA	Poly(2-hydroxy-3-aminopropyl methacrylate) microspheres with attached dithiobenzoic acid
PMPDSAH	Poly{[3-methacryloylamino)propyl]-dimethyl(3-sulfopropyl)ammonium hydroxide}
PVP	Poly( <i>N</i> -vinylpyrrolidone)
RAFT	Reversible addition-fragmentation chain transfer polymerization
SEM	Scanning electron microscopy
$\delta$	Solubility parameter ( $\text{MPa}^{1/2}$ )
$\xi$	Zeta potential (mV)

## 8. REFERENCES

- [1] Jandera P.: Separáčnı́ a analytické metody v ochraně životnı́ho prostředı́; Edice Macro M-21; Ústav makromolekulární chemie AV ČR: Praha **1996**
- [2] Arshady R.: Microspheres for biomedical applications: Preparation of reactive and labelled microspheres, *Biomaterials* **1993**, *14*, 5–15
- [3] Kawaguchi H.: Functional polymer microspheres, *Prog. Polym. Sci.* **2000**, *25*, 1171–1210
- [4] Chen H., Yuan L., Song W., Wu Z., Li D.: Biocompatible polymer materials: Role of protein-surface interactions, *Prog. Polym. Sci.* **2008**, *33*, 1059–1087
- [5] Olivier A., Meyer F., Raquez J.-M., Damman P., Dubois P.: Surface-initiated controlled polymerization as a convenient method for designing functional polymer brushes: From self-assembled monolayers to patterned surfaces, *Prog. Polym. Sci.* **2012**, *37*, 157–181
- [6] Barbey R., Lavanant L., Paripovic D., Schüwer N., Sugnaux C., Tugulu S., Klok H.A.: Polymer brushes via surface-initiated controlled radical polymerization: Synthesis, characterization, properties and applications, *Chem. Rev.* **2009**, *109*, 5437–5527
- [7] Arshady R.: Suspension, emulsion, and dispersion polymerization: A methodological survey, *Colloid Polym. Sci.* **1992**, *270*, 717–732
- [8] Dowding P.J., Vincent B.: Suspension polymerisation to form polymer beads, *Colloids Surf. A* **2000**, *161*, 259–269
- [9] Wang Q., Fu S., Yu T.: Emulsion polymerization, *Prog. Polym. Sci.* **1994**, *19*, 703–753
- [10] Šňupárek J., Formánek L.: Vodné disperze syntetických polymerů, SNTL: Praha **1979**
- [11] Harkins W.D.: A general theory of the mechanism of emulsion polymerization, *J. Am. Chem. Soc.* **1947**, *69*, 1428–1444
- [12] Okubo M.: Polymer particles, *Adv. Polym. Sci.* **2005**, *175*, 1–370
- [13] Fitch R.M.: Polymer Colloids: A Comprehensive Introduction, Academic Press: San Diego **1997**
- [14] Barret K.E.J.: Dispersion Polymerization in Organic Media, John Wiley and Sons: London **1975**
- [15] Gokmen M.T., Du Prez F.E.: Porous polymer particles – A comprehensive guide to synthesis, characterization, functionalization and applications, *Prog. Polym. Sci.* **2012**, *37*, 365–405
- [16] Shen S., Sudol E.D., El-Aasser M.S.: Dispersion polymerization of methyl methacrylate: Mechanism of particle formation, *J. Polym. Sci. A Polym. Chem.* **1994**, *32*, 1087–1100
- [17] Ober C.K., Hair M.L.: The effect of temperature and initiator levels on the dispersion polymerization of polystyrene, *J. Polym. Sci. A Polym. Chem.* **1987**, *25*, 1395–1407
- [18] Tseng C.M., Lu Y.Y., El-Aasser M.S.: Uniform polymer particles by dispersion polymerization in alcohol, *J. Polym. Sci. A Polym. Chem.* **1986**, *24*, 2995–3007
- [19] Ugelstad J., Mørk P.C., Schmid R., Ellingsen T., Berge A.: Preparation and biochemical and biomedical applications of new monosized polymer particles, *Polym. Int.* **1993**, *30*, 157–168
- [20] Zhao B., Brittain W.J.: Polymer brushes: Surface-immobilized macromolecules, *Prog. Polym. Sci.* **2000**, *25*, 677–710
- [21] Nicolas J., Guillauneuf Y., Lefay C., Bertin D., Gimes D., Charleux B.: Nitroxide-mediated polymerization, *Prog. Polym. Sci.* **2013**, *38*, 63–235
- [22] Hawker C.J., Bosman A.W., Harth E.: New polymer synthesis by nitroxide mediated living radical polymerization, *Chem. Rev.* **2001**, *101*, 3661–3688
- [23] Matyjaszewski K., Xia J.: Atom transfer radical polymerization, *Chem. Rev.* **2001**, *101*, 2921–2990

- [24] Patten T.E., Matyjaszewski K.: Copper(I)-catalyzed atom transfer radical polymerization, *Acc. Chem. Res.* **1999**, *32*, 895–903
- [25] Barner-Kowollik C.: Handbook of RAFT Polymerization, Wiley-VCH: Weinheim **2008**
- [26] Perrier S., Takolpuckdee P.: Macromolecular design via reversible addition-fragmentation chain transfer (RAFT)/xanthates (MADIX) polymerization, *J. Polym. Sci. A Polym. Chem.* **2005**, *43*, 5347–5393
- [27] Barner L., Li C., Hao X., Stenzel M.H., Barner-Kowollik C., Davis T.P.: Synthesis of coreshell poly(divinylbenzene) microspheres via reversible addition fragmentation chain transfer graft polymerization of styrene, *J. Polym. Sci. A Polym. Chem.* **2004**, *42*, 5067–5076
- [28] Rana D., Matsuura T.: Surface modification for antifouling membranes, *Chem. Rev.* **2010**, *110*, 2448–2471
- [29] Chang Y., Liao S.-C., Higuchi A., Ruaan R.-C., Chu C.-W., Chen W.-Y.: A highly stable nonbiofouling surface with well-packed grafted zwitterionic polysulfobetaine for plasma protein repulsion, *Langmuir* **2008**, *24*, 5453–5458
- [30] Rodriguez-Emmenegger C., Brynda E., Riedel T., Houska M., Šubr V., Alles A.B., Hasan E., Gautrot J.E., Huck W.T.S.: Polymer brushes showing non-fouling in blood plasma challenge the currently accepted design of protein resistant surfaces, *Macromol. Rapid Commun.* **2011**, *32*, 952–957
- [31] Lowe A.B., McCormick C.L.: Polyelectrolytes and Polyzwitterions: Synthesis, Properties, and Applications, ACS: Washington **2006**
- [32] Schlenoff J.B.: Zwitteration: Coating surfaces with zwitterionic functionality to reduce nonspecific adsorption, *Langmuir* **2014**, *30*, 9625–9636
- [33] West S.L., Salvage J.P., Lobb E.J., Armes S.P., Billingham N.C., Lewis A.L., Hanlon G.W., Lloyd A.W.: The biocompatibility of crosslinkable copolymer coatings containing sulfobetaines and phosphobetaines, *Biomaterials* **2004**, *25*, 1195–1204
- [34] Zhao C., Zhao J., Li X., Wu J., Chen S., Chen Q., Wang Q., Gong X., Li L., Zheng J.: Probing structure-antifouling activity relationships of polyacrylamides and polyacrylates, *Biomaterials* **2013**, *34*, 4714–4724
- [35] Larkin P.: Infrared and Raman Spectroscopy: Principles and Spectral Interpretation, Elsevier: San Diego **2011**, pp. 31–44
- [36] Delgado A.V., González-Gaballero F., Hunter R.J., Koopal L.K., Lyklema J.: Measurement and interpretation of electrokinetic phenomena, *Pure Appl. Chem.* **2005**, *77*, 1753–1805
- [37] Horák D., Shapoval P.: Reactive poly(glycidyl methacrylate) microspheres prepared by dispersion polymerization, *J. Polym. Sci. A Polym. Chem.* **2000**, *38*, 3855–3863
- [38] Lok K.P., Ober C.K.: Particle size control in dispersion polymerization of polystyrene, *Can. J. Chem.* **1985**, *63*, 209–216
- [39] Koubková J., Horák D.: Poly(glycidyl methacrylate) microspheres: Preparation of poly-(acrylic acid)-stabilized dispersion polymerization and effect of some reaction parameters, *J. Colloid Sci. Biotechnol.* **2013**, *2*, 218–225
- [40] Liu Y., He J., Xu J., Fand D., Tang W., Yang Y.: Thermal decomposition of cumyl dithiobenzoate, *Macromolecules* **2005**, *38*, 10332–10335
- [41] Parker R.E., Isaacs N.S.: Mechanisms of epoxide reactions, *Chem. Rev.* **1959**, *59*, 737–799
- [42] Yoshikawa C., Goto A., Tsujii Y., Fukuda T., Yamamoto K., Kishida A.: Fabrication of high-density polymer brush on polymer substrate by surface-initiated living radical polymerization, *Macromolecules* **2005**, *38*, 4604–4610

- [43] Carey F.A., Sundberg R.J.: *Advanced Organic Chemistry: Structure and Mechanisms*, 5<sup>th</sup> Edition, Springer: New York **2007**, pp. 389–472
- [44] Cho W.K., Kong B., Choi I.S.: Highly efficient non-biofouling coating of zwitterionic polymers: Poly[(3-(methacryloylamino)propyl)-dimethyl(3-sulfopropyl)ammonium hydroxide], *Langmuir* **2007**, *23*, 5678–5682
- [45] Li Q., Zhou B., Bi Q.-Y., Wang X.-L.: Surface modification of PVDF membranes with sulfobetaine polymers for a stable anti-protein-fouling performance, *J. Appl. Polym. Sci.* **2012**, *125*, 4015–4027
- [46] Lee W.-F., Tsai C.-C.: Synthesis and solubility of the poly(sulfobetaine)s and the corresponding cationic polymers: 1. Synthesis and characterization of sulfobetaines and the corresponding cationic monomers by nuclear magnetic resonance spectra, *Polymer* **1994**, *35*, 2210–2217
- [47] Monroy Soto V.M., Gailn J.C.: Poly(sulphopropylbetaines): 2. Dilute solution properties, *Polymer* **1984**, *25*, 254–262
- [48] Li C., Han J., Ryu C.Y., Benicewicz B.C.: A versatile method to prepare RAFT agent anchored substrates and the preparation of PMMA grafted nanoparticles, *Macromolecules* **2006**, *39*, 3175–3183
- [49] Li C., Benicewicz B.C.: Synthesis of well-defined polymer brushes grafted onto silica nanoparticles via surface reversible addition-fragmentation chain transfer polymerization, *Macromolecules* **2005**, *38*, 5929–5936
- [50] Vien D.L., Colthup N.B., Fateley W.G. Grasselli J.G.: *The Handbook of Infrared and Raman Characteristic Frequencies of Organic Molecules*, Academic Press: New York, **1991**
- [51] Silverstein R.M., Bassler G.C., Morrill T.C.: *Spectrometric Identification of Organic Compounds*, 5<sup>th</sup> Edition, John Wiley & Sons: New York **1991**, pp. 91–131
- [52] Polzer F., Heigl J., Schneider C., Ballauff M., Borisov O.V.: Synthesis and analysis of zwitterionic spherical polyelectrolyte brushes in aqueous solution, *Macromolecules* **2011**, *44*, 1654–1660
- [53] Wu L., Jasinski J., Krishnan S.: Carboxybetaine, sulfobetaine, and cationic block copolymer coatings: A comparison of the surface properties and antibiofouling behaviour, *J. Appl. Polym. Sci.* **2012**, *124*, 2154–2170,
- [54] Mary P., Bendejacq D.D., Labeau M.-P., Dupuis P.: Reconciling low- and high-salt solution behaviour of sulfobetaine polyzwitterions, *J. Phys. Chem. B* **2007**, *111*, 7767–7777
- [55] Czeslik C., Jackler G., Steitz R., Grünberg H.H.: Protein binding to like-charged polyelectrolyte brushes by counterion evaporation, *J. Phys. Chem. B* **2004**, *108*, 13395–13402
- [56] Kaufman E.D., Beleyea J., Johnson M.C., Nicholson Z.M., Ricks J.L., Shah P.K., Byales M., Pettersson T., Feldotö Z., Blomberg E., Claesson P., Franzen S.: Probing protein adsorption onto mercaptoundecanoic acid stabilized gold nanoparticles and surface by quartz crystal microbalance and  $\xi$ -potential measurements, *Langmuir* **2007**, *23*, 6053–6062
- [57] Roth C.M., Lenhoff A.M.: Electrostatic and van der Waals contributions to protein adsorption: Computation of equilibrium constants, *Langmuir* **1993**, *9*, 962–972
- [58] Shao Q., He Y., White A.D., Jiang S.: Difference in hydration between carboxybetaine and sulfobetaine, *J. Phys. Chem. B* **2010**, *114*, 11625–11631

## 9. LIST OF AUTHOR PUBLICATIONS

### Journals

- Koubková J., Horák D.: Poly(glycidyl methacrylate) microspheres: Preparation of poly(acrylic acid)-stabilized dispersion polymerization and effect of some reaction parameters, *J. Colloid Sci. Biotechnol.* **2013**, 2, 218–225
- Koubková J., Müller P., Hlídková H., Plichta Z., Proks V., Vojtěšek B., Horák D.: Magnetic poly-(glycidyl methacrylate) microspheres for protein capture, *New Biotechnol.* **2014**, 31, 482–491
- Golunova A., Chvátil D., Krist P., Kotelnikov I., Abelová L., Kotek J., Sedlačík T., Kučka J., Koubková J., Studenovská H., Rypáček F., Proks, V.: Toward structured macroporous hydrogel composites: Electron beam initiated polymerization of layered cryogels, *Biomacromolecules*, submitted

### Posters and presentation

- Koubková J., Horák D.: Zwitterion-grafted poly(glycidyl methacrylate) microspheres using RAFT polymerization; Frontiers of Polymer Colloids: From Synthesis to Macro-Scale and Nano-Scale Applications. 78<sup>th</sup> Prague Meeting on Macromolecules, Prague 2014, Czech Republic, Book of Abstracts, p. 133
- Koubková J., Proks V., Trchová M., Horák D.: Monodisperse poly(glycidyl methacrylate) microspheres coated with zwitterionic polymers; Novel Technologies for In Vitro Diagnostics DIATECH 2014, 2014, Leuven, Belgium, Book of Abstracts, p. 14
- Proks V., Golunova A., Chvátil D., Krist P., Kotelnikov I., Abelová L., Kotek J., Sedlačík T., Kučka J., Koubková J., Studenovská H., Rypáček F.: Strukturované makroporézní hydrogely: kryogelace akrylamidů iniciovaná elektronovým svazkem, Československá konference POLYMERY 2014, 2014, Třešť, Česká republika